scientific reports

OPEN

Particle shape analysis of calcareous sand based on digital images

Xiaobing Wei[2✉], Yani Lu[1,3], Xiaoxuan Liu[4], Biwen Zhang[4], Mingxing Luo[1,3] & Li Zhong[1,3✉]

Particle geometric is a key parameter that defines the eometric attributes of calcareous sand particles and is intricately related to their mechanical traits, such as compression and shear. The scanning electron microscopy and digital imaging were applied to capture the microscopic properties and geometric projections of calcareous sand. The qualitative analysis, conventional statistical methods and fractal theory were employed to describe the geometric morphology of sand particles. Additionally, we analyzed the structural and physical traits of calcareous sand based on its unique biological genesis. We developed a hypothetical structural-physical model for calcareous sand. Our findings revealed the interwoven reticulation on the surface of calcareous gravel particles, along with an uneven distribution of pores on the external surface. As the particle size increased, the global profile factor decreased and the angularity increased. The critical threshold for the variations in flatness, surface roughness, and circularity was observed at a particle size of 5 mm, with the particle size having a relatively minor effect on these characteristics for particles smaller than 5 mm. The shape of the calcareous sand particles exhibited fractal characteristics, with fractal dimension serving as a measure of surface smoothness, particle breakage, and strength. These experimental results could significantly enhance our understanding of the mechanical behavior of calcareous sand.

Calcareous sand, a granular material primarily composed of marine biogenic calcium carbonate exceeding 90%, exhibits distinctive traits including high angularity, abundant internal pores, irregular shape, low strength, and fragility[1]. Hence, their engineering mechanical properties diverge significantly from those of typical terrestrial and marine sediments. Analyzing the particle geometry is imperative for characterizing the unique geometric features of calcareous sand. In non-cohesive soils, such as sand and rockfill materials, the particle shape demonstrates the close relationship with mechanical properties, such as compression and shear, indicating its crucial role in assessing engineering mechanical properties.

The shear resistance of a granular material can be affected by the cementation properties, interparticle friction, and particle shape. For uncemented granular materials, the shear strength relies on certain factors such as friction, particle rearrangement, interlocking (dilatancy), and particle breakage[2]. The particle shape is the dominant factor influencing the particle spatial arrangement, occlusion, and breakage. Therefore, a systematic evaluation of the particle shape can enhance the analysis of the mechanical behavior of calcareous sand.

Chon et al.[3] investigated the impact of particle morphology on the stiffness and strength of large sandy soil databases and visually assessed the sand particle sphericity and roundness using two-dimensional fine-scale images. Koerner[4] explored the impact of angularity, gradation, and mineralogy on the shear strength of cohesionless soils, demonstrating that the angle of internal friction increased with increasing in the particle angularity and declined as the effective particle size increased. Hyslip et al.[5] employed fractal dimension to characterize the natural similarity of gravel morphology across multiple observation scales. Zhu et al.[6] examined and quantified the internal pore distribution using laser cutting in their experiments. Zhu et al.[7] classified the internal pore shapes according to the pore shape coefficient K_f that measured the ratio of the equal area perimeter to the actual pore perimeter. Wang[8] employed the electron microscopy to determine the roundness, ring-to-diameter ratio,

[1]School of Civil Engineering, Hubei Engineering University, Xiaogan 432000, Hubei, China. [2]Zhejiang Zhongjiao Tongli Engineering Design Co. LTD, Hangzhou 310000, Zhejiang, China. [3]Hubei Small Town Development Research Center, Hubei Engineering University, Xiaogan 432000, Hubei, China. [4]School of Civil Engineering and Architecture, Wuhan University of Technology, Wuhan 430070, Hubei, China. ✉email: 18657128993@163.com; zhongl@hbeu.edu.cn

circularity, and roughness of calcareous sands. The findings revealed a ring-to-diameter ratio ranging between 1 and 3, with the particle shapes predominantly characterized by lumps and fusiforms.

Using the scanning electron microscopy (SEM), Jiang[9] observed that the calcareous sand surfaces exhibited numerous fine pores. They suggested that these internal pores contributed to particle breakage under low stress. Chen[10] adopted the statistical methods and fractal theory to analyze the particle shape of calcareous sand. The results revealed that the calcareous sand exhibited fractal particle shape characteristics, with fractals becoming more pronounced as, the particle size decreased[11]. Alshibli et al.[12] utilized the three-dimensional simultaneous microcomputed tomography (SMT) to obtain the high-resolution three-dimensional particle shape indices for granular soils, including quartz sand and calcareous sand, discovering a correlation between the particle shape and shear strength. Jiang et al.[13] analyzed SEM images of calcareous sand using the Matlab image processing, concluding that the internal pore presence in the calcareous sand particles was independent of particle shape but closely linked to particle size. Zhou et al.[14] employed the X-ray and μCT scanning techniques to capture tomography images of calcareous sand, revealing a stronger fractal characteristic within the internal pores with a positive correlation between the internal void ratio and fractal dimension. Wang et al.[15] analyzed the projected shapes of these particles in various orientations using the Partan system, thereby characterizing the morphology of calcareous sand and proposing a classification method for its shape. Li et al.[16] utilized the computer tomography to characterize the three-dimensional particle breakage of calcareous sand. Their findings suggested that the calcareous sand particles exhibited the angularity, low sphericity, and susceptibility to breakage. Moreover, particles with high void ratios demonstrate increased fracture susceptibility. Cui et al.[17] investigated the properties of unique pores in calcareous sand through a range of microscopic research methods, concluding that the particle shape and surface roughness were the main factors influencing the pore shape, pore radius, and pore connectivity. Current studies on the shape of calcareous sand particles have primarily focused on the qualitative descriptions, whereas the systematic analysis of the impact of particle size remains unexplored.

The main methods for studying and evaluating the particle shape through particle images are digital image analysis and identification, scanning electron microscopy (SEM), CT scanning, etc. For digital image analysis and identification, color images taken by digital cameras are stored in RGB format. Since each pixel information in the image in this format consists of three color degrees of blue, red and green channels, digital image preprocessing is required to take into account the effects of various factors such as camera and environment on imaging. Image software such as PhotoShop, IPP, etc. are usually used to grayscale color images to increase the brightness and contrast of the image, so as to improve the difference between the binary media. Then, the picture is binaryized through grayscale analysis (the pixels representing the medium are distinguished, so that the digital image information is converted to the fine structure modeling information), and the positions of the corresponding pixels are exported, and the relevant information of the medium is obtained after processing by the digital image processing software. This method is simple and easy to implement, and can truly reflect the particle composition of the whole specimen, but the human factor has a greater impact. Scanning electron microscope (SEM) is through the magnification technology to obtain the image of a certain side of the particle. Quantitative particle analysis is performed through the image, but the analyzed particles are limited, mostly the particle microscopic observation is performed. CT scanning is a combination of imaging techniques to obtain images of different sections of the specimen. The images are used for the quantitative particle analysis. In this study, due to the limitations of the test conditions, digital image analysis and identification is used for particle shape analysis.

In this study, SEM and digital images were obtained to analyze the surface morphology characteristics of calcareous sand through experimentation. The quantitative particle shape data were extracted from the images using digital processing and statistical analyses. The shape distributions across various particle sizes were examined to facilitate a quantitative description of calcareous sand morphology. Furthermore, the analysis of the calcareous sand characteristics was combined with its unique biological genesis.

Quantification of particle shape

The particle shape quantification in calcareous sands can be achieved through the accurate identification of medium information and statistical analysis of the conventional geometric data. These methods can be categorized into the qualitative and quantitative methods. The qualitative methods refers to visually assessing the particle geometry based on vision and experience. Specialized terms such as spherical, flaky, and dendritic are commonly employed to describe particle shape. However, these terms are too subjective and may not accurately depict the particle morphology[15,18]. The quantitative methods utilize the shape geometry data to define various shape indices such as the global profile factor and roundness. The descriptions are crucial in engineering owing to their reproducibility. Typically, five common quantitative shape indices can be employed to evaluate the particle morphology.

(1) *The global profile factor α* generally represents the ratio of the equivalent area circumference of the two-dimensional projected contour of a particle to the actual circumference of the two-dimensional projected boundary contour of the particle. For a standard circular particle, the global profile factor **α** equal to 1. Consequently, the global profile factor value is always less than or equal to 1.

(2) *The flatness β* is the ratio of the largest Feret diameter to the smallest diameter in the two-dimensional projected contour of the particle. It denotes the narrowness of the particles, and its value can be always higher or equal to 1. The flatness **β** value can increase when the particles are flatness and narrower.

(3) *The circularity φ* is the ratio of the largest tangent circle radius to the smallest external circle radius of the two-dimensional projected contour of the particle. It represents the fitting degree between the overall shape of the two-dimensional projected contour of the particle and the standard circle and the fitting

degree of the length, width and height dimensions of the two-dimensional projected contour of the particle. When the actual particle shape deviates from a circle, φ can be smaller.

(4) *The angularity ψ* is the ratio of the perimeter of the smallest external polygon along the particle contour to the perimeter of its equivalent ellipse. The equivalent ellipse denotes a standard ellipse with the same area and flatness as the particle projection. When the particle surface features a greater number of angles with more pronounced prominence, the angularity ψ value can increase.

(5) *The surface roughness χ* denotes the square of the ratio of the perimeter of the two-dimensional projected contour of the particle to the perimeter of the smallest external polygon along the particle contour. When the surface of the particle was rougher and exhibited greater irregularity and boundary undulation, the surface roughness (χ) value could increase. In the parameter definitions provided above, the effective diameter of the particle was determined by drawing lines through the object's center of mass at 2° intervals and averaging all these lines to obtain the effective diameter of the object, as illustrated in Fig. 1a. The corresponding geometric schematic of each parameter is shown in Fig. 1b.

Fractal geometry has emerged as a practical method for measuring irregular particle shapes in particle shape analysis[11]. The term "Fractal" was coined by Mandelbrot who established the concept of Fractal Geometry. This method is applicable for describing the shape characteristics of calcareous sand in terms of fractal dimension. As fractal dimension quantitatively represents the figure complexity, it can characterize the degree of concavity and convexity of the projected contour lines of the particles, thereby representing the particle shape. For example, the shape fractal dimension strongly correlates with the global profile factor. When the particle surface is smoother, the concave and convex features in the projected contour lines can be fewer. Accordingly, the fractal dimension D decreases, while the global profile factor increases and approaches 1. Fractal dimensions, commonly used for particle shape determination, can be categorized into two types: the variable scale method and the fixed scale method.

(1) *Variable-scale method* The definition is based on the concept that the particle circumference L is determined using measurements at a scale ε, ignoring the irregularities smaller than ε, A series of perimeters can be obtained by systematically varying the measurement scale. By plotting these on a double logarithmic curve, the slope can yield the parameter K, from which the fractal dimension D of the particle shape can be derived as.

$$D = 1 - K \tag{1}$$

(2) *Fixed-scale method* This definition is based on the idea that both the perimeter and area of a particle are calculated using the same measurement scale ε. For a geometric plane of irregular shape, fractal dimension adheres to the following equation:

$$L(\varepsilon) \propto A(\varepsilon)^{D/2} \tag{2}$$

The slope, denoted by K, can be determined by plotting double logarithmic curve. Fractal dimension D of the particle shape is twice the slope of this straight line:
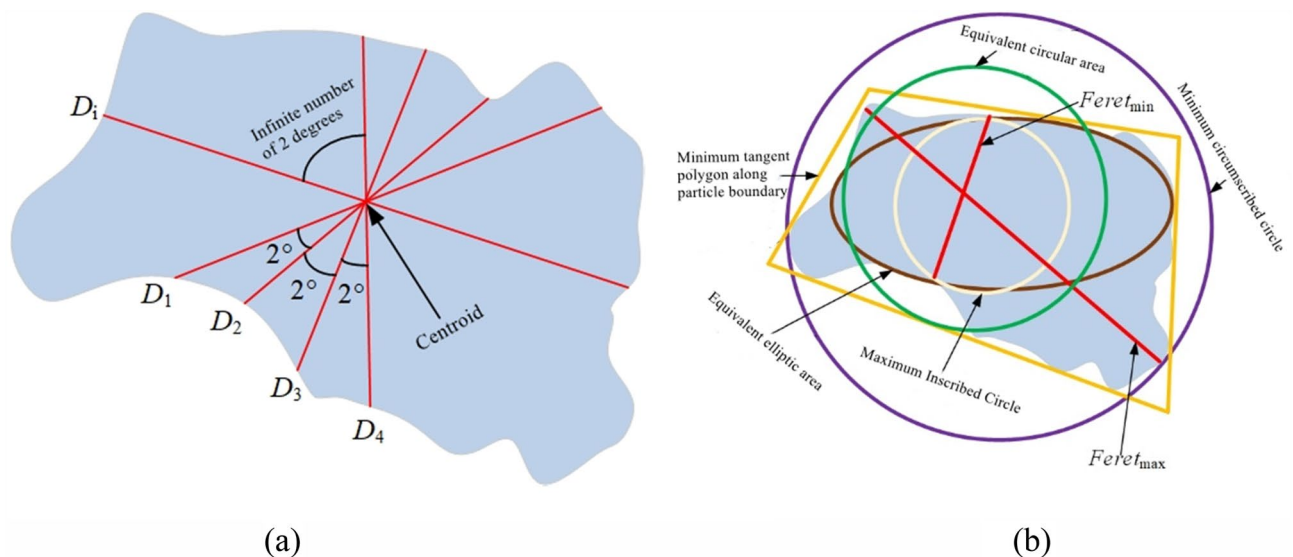
$$D = 2K \tag{3}$$

Figure 1. Definition of parameters related to particle shape (**a**) Schematic diagram of particle effective diameter (**b**) Schematic diagram of basic size parameters.

The analysis demonstrates that both qualitative and quantitative methods can describe the particle shape. In this study, the shape of calcareous sand particles was examined using SEM imaging method, conventional statistical method, and fractal theory in an experimental setting. Given that the variable scale method required the change in the measurement scale, fractal dimension measurements were conducted using the fixed-scale method for ease of measurement.

Particle shape analysis test

The calcareous sand sourced from the Yongshu Reef in the Nansha Islands served as the test material. It was composed by the loose coral clastic sediment without cementation, with the calcium carbonate as the primary constituent. Before the test, the sand specimens were washed with distilled water to eliminate the salt content and dried for further applications. To investigate the distribution of connected pores among calcareous sand particles of varying sizes and shapes, the specimens were categorized into the following particle size groups: > 20 mm, 10–20 mm, 5–10 mm, 2–5 mm, 1–2 mm, 0.5–1 mm, 0.25–0.5 mm, 0.1–0.25 mm, and 0.074–0.1 mm. The test methods were divided into two categories.

(1) The qualitative description of SEM images. SEM model JSM-5610LV, manufactured by Nippon Electronics Corporation, was adopted for the test. The nine groups of calcareous sand, ranging in particle size from 0.074 to 20 mm, were randomly selected and magnified at 50, 500, and 5000 times for the qualitative observation.

(2) The conventional statistical methods. The two groups, labeled Group A and Group B were randomly selected from the same calcareous sand sample. Additionally, the seven groups of calcareous sand, spanning particle sizes ranging from larger than 20 mm, 10–20 mm, 5–10 mm, 2–5 mm, 1–2 mm, 0.5–1 mm, and 0.25–0.5 mm, were selected for analysis. The quantities and particle sizes of each specimen group are listed in Table 1. The statistical analysis indicated that Group A contained 299 particles, and Group B contained 550 particles. The particles count was limited because of the extensive surface area of the larger particles and their wide spatial distribution. First, the sand specimens were uniformly spread over a pre-positioned black workbench with a reference positioned on the bottom plate. In the case of particle contact the tweezers were employed to delicately dislodge them, thereby preventing the introduction of artificial data processing errors caused by the test inaccuracies. Subsequently, the high-resolution digital images of calcareous sand specimens were captured using a digital camera. Finally, Image-Pro Plus image processing software was applied to analyze and identify the digital images. All the collected images were then analyzed to extract the relevant particle shape indices and fractal dimensions. Considering certain factors such as the quantity of test particles, number of tests conducted, and human influences, a change in test personnel was implemented. Subsequently, 144 calcareous sand particles from each of the two particle size ranges (0.5–1 mm and 0.25–0.5 mm) utilized in the tests were randomly selected for the parallel tests with the testers replaced. The similarity observed in relevant particle shape parameters between the two test results suggested the representativeness of the findings of this study.

Results and analysis
Qualitative description of SEM images

Figure 2 illustrates the calcareous sand particles. The visual inspection of the calcareous sand particles revealed that the pure calcareous sand specimens appeared white, with individual particle surfaces adorned with dark red or gray minerals. The observations of the particle shape indicated a diverse range, including lumpy, spherical, fusiform, lamellar, dendritic, polygonal, and others. Santamarina et al.[19] proposed a three-scale characterization of soil particle shape, comprising sphericity, angularity, and roughness. The first scale parameter primarily characterized the overall particle shape, described as the spherical, massive, or columnar. The second scale parameter characterized the angular features, expressed in terms of angularity or roundness, and the third scale parameter denoted the surface texture and undulation degree, described as roughness. Although the quantitative depiction of the particle morphology across the three scales has been widely acknowledged within the academic

Group	Particle size	Number (pcs)	Group	Particle size	Number (pcs)
Group A	Larger than 20 mm	7	Group B	Larger than 20 mm	6
	10–20 mm	15		10–20 mm	16
	5–10 mm	15		5–10 mm	20
	2–5 mm	40		2–5 mm	60
	1–2 mm	56		1–2 mm	104
	0.5–1 mm	71		0.5–1 mm	187
	0.25–0.5 mm	95		0.25–0.5 mm	157
Total		299	Total		550

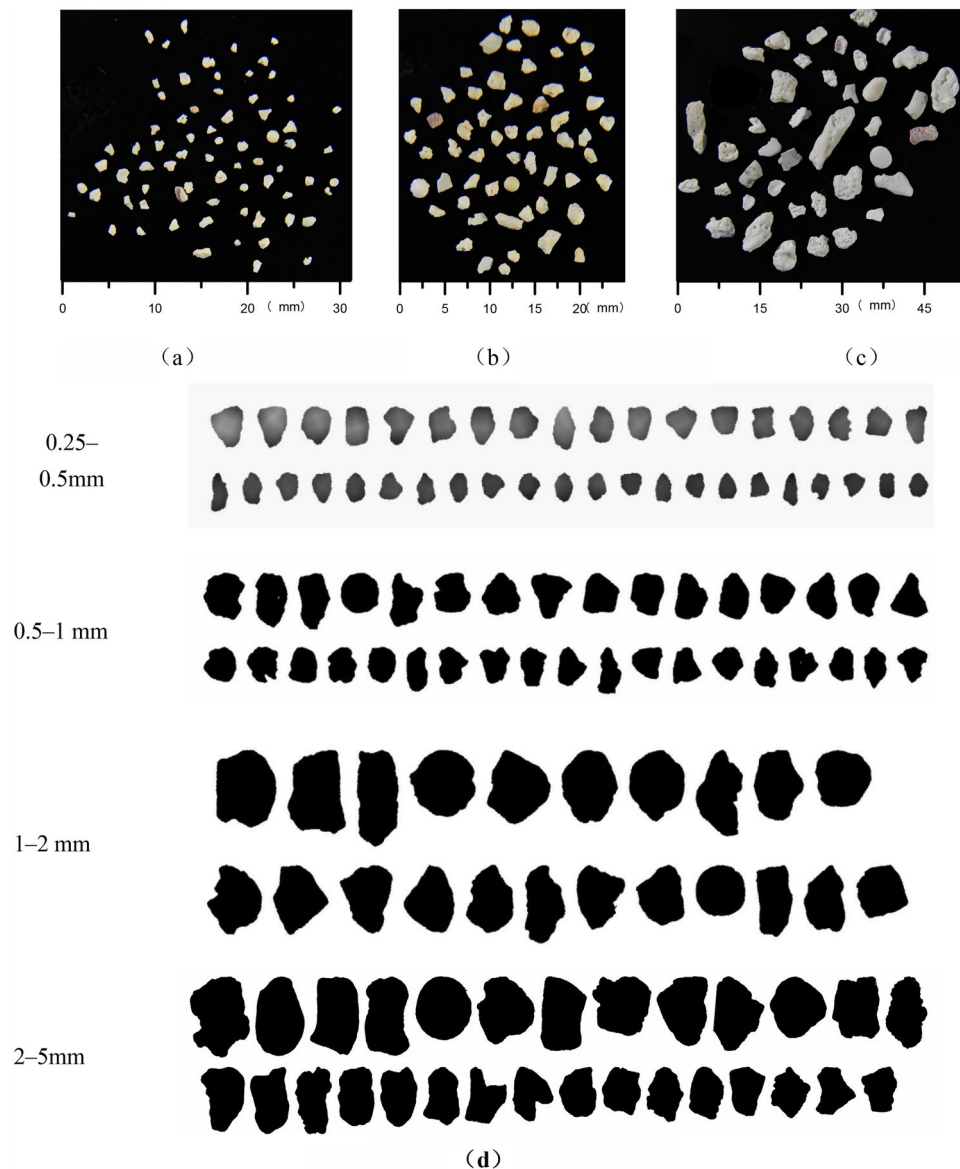**Table 1.** Summary of the number of particles in each group.

Figure 2. Calcareous sand particles (**a**) 0.5–1 mm specimen (**b**) 1–2 mm specimen (**c**) 2–5 mm specimen (**d**) A series of images of particles.

community, studies have reported various definitions of the quantitative parameters to describe the particle morphology[20–23]. For example, Krumbein[24] categorized the pebble particle shapes into four types, including disc-shaped, spherical, razor-sharp, and rod-shaped, based on the width-to-length and thickness-to-width ratios. The sphericity was determined by the length ratio of the particles across the three mutually orthogonal axes via manual measurements. The powers[25] employed naked-eye observation and comparative methods to classify the particle morphology, classifying the roundness into six grades and sphericity into two grades.

The surfaces of the calcareous sand particles exhibited certain prominent features, including a honeycomb-like pockmarked surface with irregularities, numerous pits and holes, and an abundance of cracks and defects. Larger particles notably demonstrated evident angles, low roundness, high angularity, abundant internal pores and retained the morphology of protozoan organisms. The dried and cooled calcareous sand specimens were placed on paper and a small amount of pure water was added using a rubber-tipped burette. The rapid absorption of water by the calcareous sand and immediate wetting of this study indicated a certain degree of pore connectivity within the particles. Moreover, the particles of different sizes exhibited distinct shapes. For the smaller particles, the shapes were primarily lumps, spheres, flakes, and fusiforms. The particle structure exhibited a greater density, with less complex and more regular shapes. The pores within these particles were challenging to identify with naked eyes. Certain flaky structures exhibited low strength, were easily pressed off with fingernails, and demonstrated rough cross sections. Conversely, as the particle size increased, the shapes became predominantly dendritic and blocky with a noticeable increase in the aspect ratio and visibility of the pores. The particle shapes became more complex with increased strength, making it difficult for them to break with fingers.
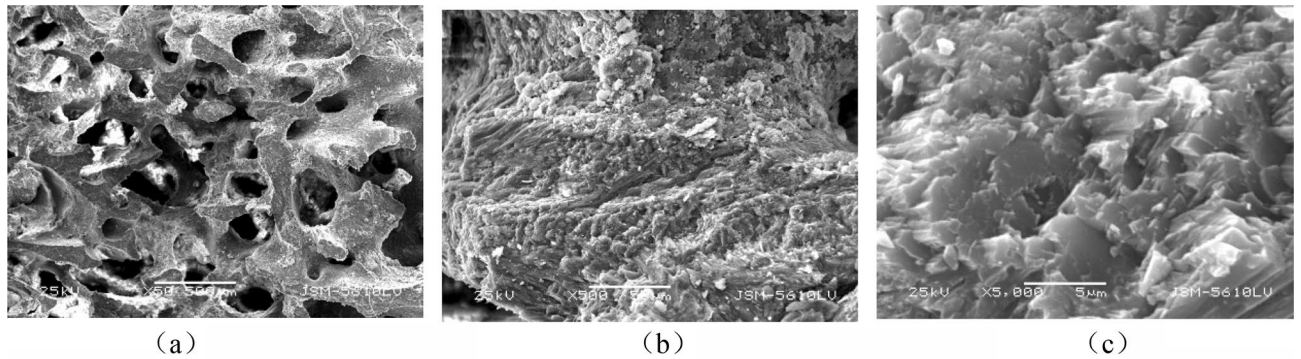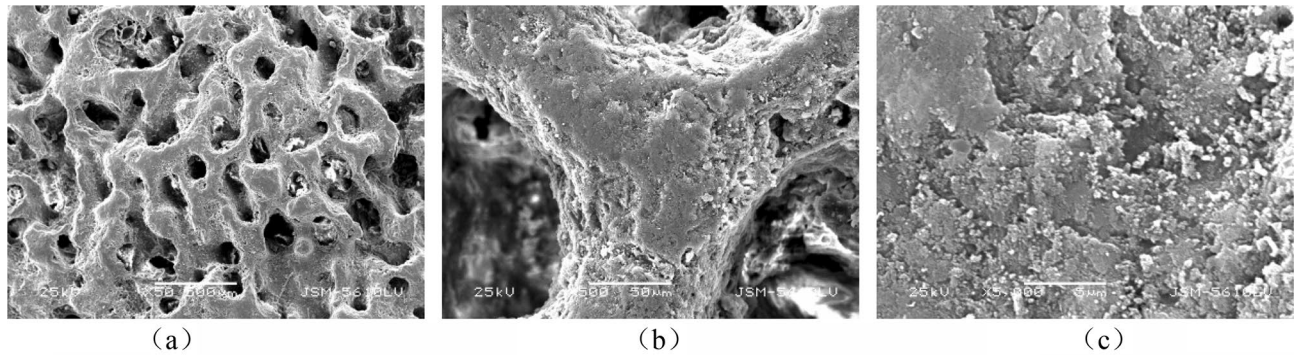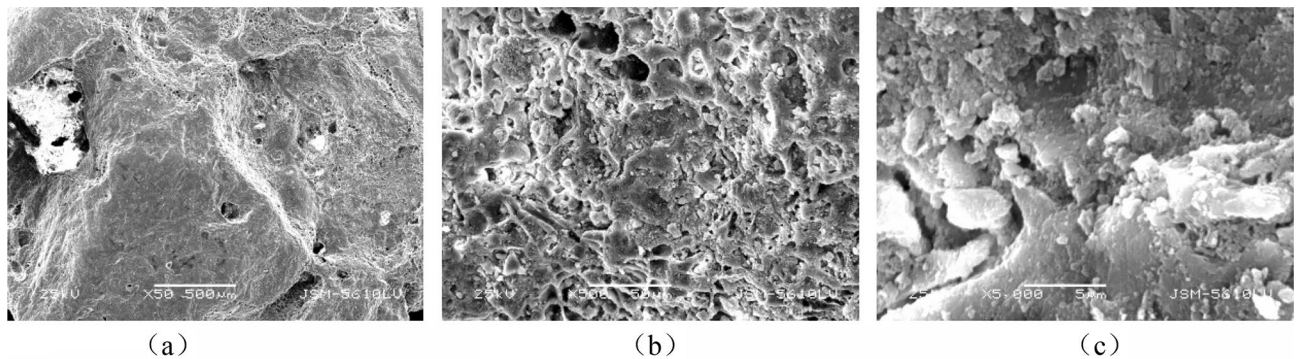
Figure 3. Scanning electron microscopy (SEM) images of particle sizes within the range of 10–20 mm at different magnifications (**a**) 50 times magnification (**b**) 500 times magnification (**c**) 5000 times magnification.

Figure 4. Scanning electron microscopy (SEM) images of particle sizes within the range of 5–10mm at different magnifications (**a**) 50 times magnification (**b**) 500 times magnification (**c**) 5000 times magnification.

Figure 5. Scanning electron microscopy (SEM) images of particle sizes within the range of 2–5 mm at different magnifications (**a**) 50 times magnification (**b**) 500 times magnification (**c**) 5000 times magnification.

SEM images of each particle size are shown in Figs. 3–11. As shown in Figs. 3–5, the calcareous gravel particles exhibited the intertwined reticulation morphology on the surface at lower magnifications. Within the range between 5 and 20 mm, the particle reticular skeleton morphology became more pronounced, with an increased presence of inhomogeneous surface pores. Larger particle sizes corresponded to more numerous and larger surface pores. At higher magnifications, the particle surfaces appeared uneven and exhibited high roughness, and the particles were formed by the aggregation of numerous irregularly shaped crystals. As shown in Figs. 6–10, the calcareous coarse particles indicated an increased pore count, angularity, and significant shape disparities at lower magnifications. Conversely, the particle size reduction corresponded to a gradual decrease in the shape disparities. Similar to calcareous gravel particles, the particles comprised fine crystals with tumbled surfaces and high roughness at high magnifications. As shown in Fig. 11, the shape disparities between the finer particles beneath the calcareous coarse particles decreased. However, even at a magnification of 5000 times, the surface pores were
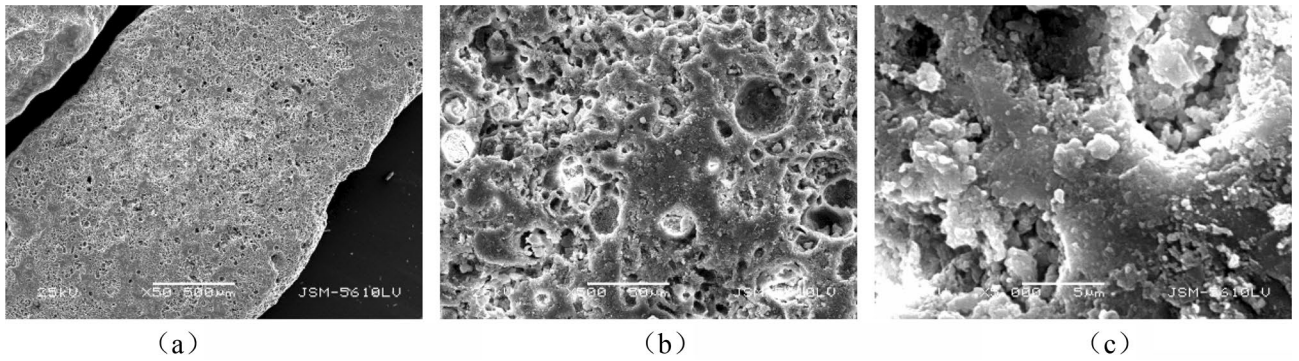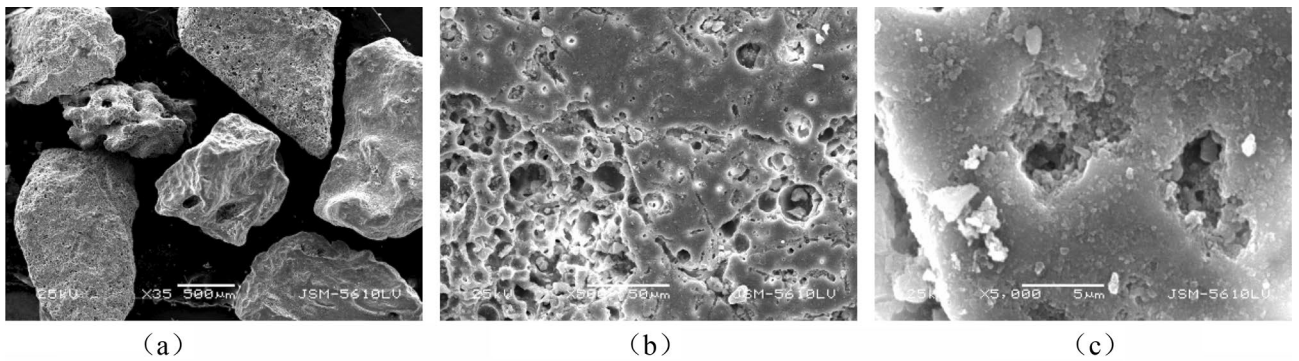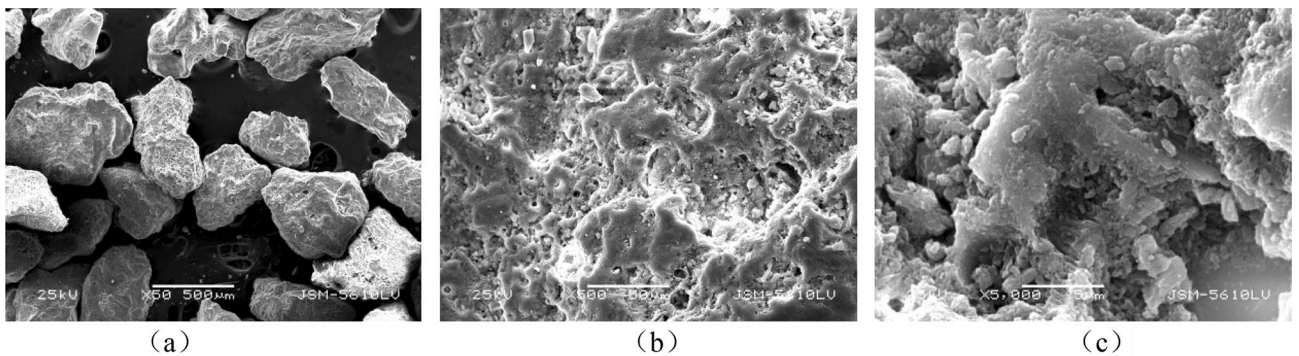
Figure 6. Scanning electron microscopy (SEM) images of particle sizes within the range of 1–2mm at different magnifications (**a**) 50 times magnification (**b**) 500 times magnification (**c**) 5000 times magnification.

Figure 7. Scanning electron microscopy (SEM) images of particle sizes within the range of 0.5–1mm at different magnifications (**a**) 50 times magnification (**b**) 500 times magnification (**c**) 5000 times magnification.

Figure 8. Scanning electron microscopy (SEM) images of particle sizes within the range of 0.25–0.5mm at different magnifications (**a**) 50 times magnification (**b**) 500 times magnification (**c**) 5000 times magnification.

still evident in the particles, in contrast to the surface morphology of the majority of particles. This observation revealed the distinctive microscopic morphology of the calcareous fine particles within this particle size range.

The comprehensive analysis revealed the following characteristics of calcareous sand particles. The calcareous gravel particles exhibited an interwoven reticulation on the surface, with an uneven distribution of external surface pores. Each particle group presented a higher number of pores on the external surface, and the larger particles exhibited more pronounced external surface pores. As the particle size decreased, the shape disparities were reduced, accompanied by a gradual reduction in the angularity. The rough and uneven surfaces of particles may result in increased occlusion and friction forces between particles when subjected to external forces, leading to the particle breakage or surface abrasion and the generation of smaller particles. The fine particles smaller than 0.074 mm exhibited the external surface pores under high magnification.
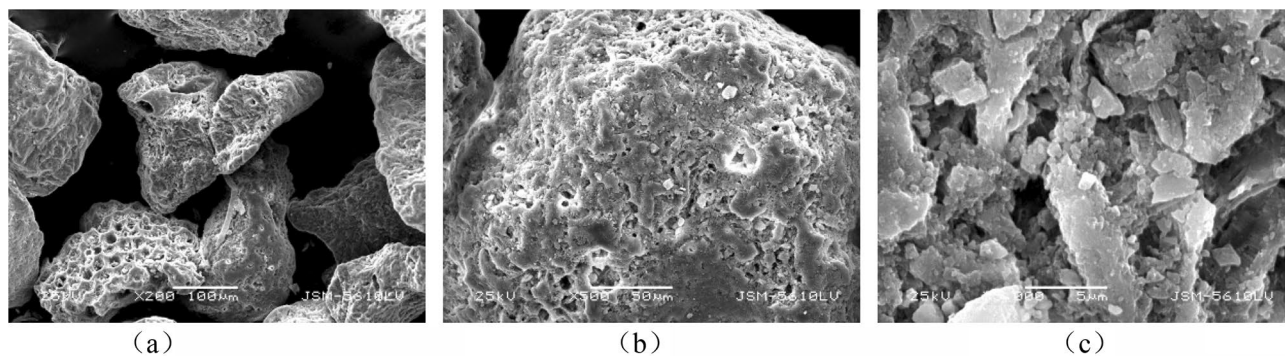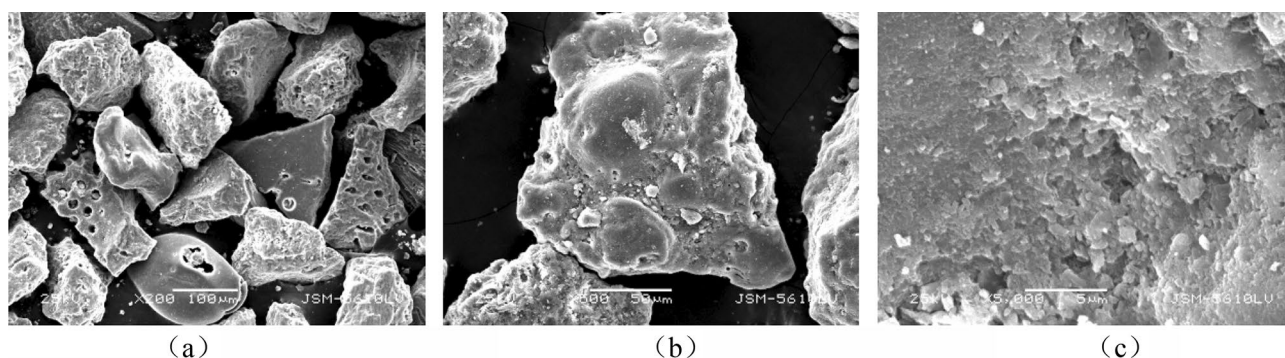
(a)　　　　　　　　　　　(b)　　　　　　　　　　　(c)

Figure 9. Scanning electron microscopy (SEM) images of particle sizes within the range of 0.1–0.25 mm at different magnifications (**a**) 50 times magnification (**b**) 500 times magnification (**c**) 5000 times magnification.
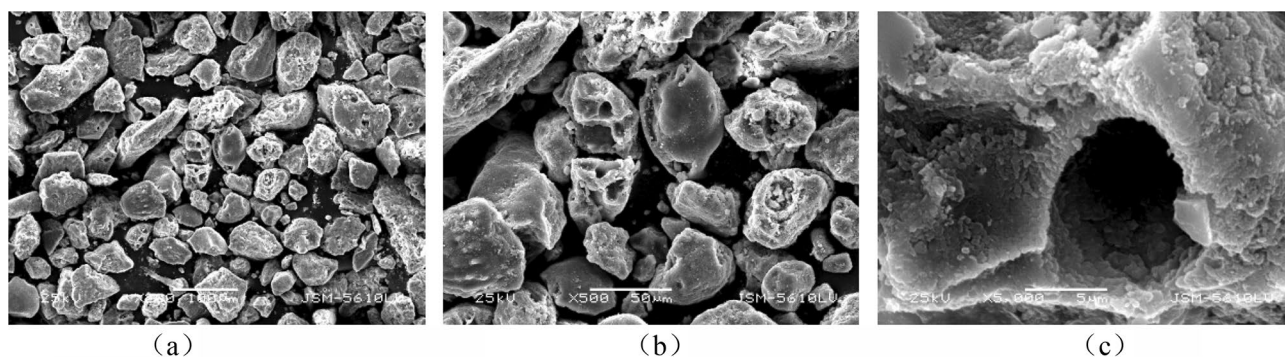

(a)　　　　　　　　　　　(b)　　　　　　　　　　　(c)

Figure 10. Scanning electron microscopy (SEM) images of particle sizes within the range of 0.074–0.1 mm at different magnifications (**a**) 50 times magnification (**b**) 500 times magnification (**c**) 5000 times magnification.

(a)　　　　　　　　　　　(b)　　　　　　　　　　　(c)

Figure 11. Scanning electron microscopy (SEM) images of particle sizes less than 0.074mm at different magnifications (**a**) 50 times magnification (**b**) 500 times magnification (**c**) 5000 times magnification.

Structural-physical modeling

The calcareous sands deposited without extensive transportation retain small voids in their primary bioskeletons, resulting in the particles with multiple voids and irregular shapes. Coupled with Figs. 3–11, the fine morphology highlighted the calcareous sand particles with uneven surfaces, numerous pits and holes, an intertwined reticulation morphology, multiple cracks and defects, distinct edges and angles, low roundness, high angularity, and abundant internal pores. The compositional analysis and fundamental petrographic knowledge revealed that the calcareous sand particles primarily relied on $CaCO_3$ to form the particle matrix. Larger-diameter particles were dependent on the finer mineral particles to create the calcareous sand. Nonetheless, insufficient or incomplete cementation contributed to numerous connected or disconnected pore structures within internal and external matrices.

As reported by Zhu et al.[26], the observations of the thin sections and SEM images indicated that the matrix cementation of calcareous sand can be classified into two types: (1) Contact cementation consisting of granular calcite, acicular aragonite and biotite microcrystals. (2) Mosaic cementation involving the biogenic microcrystals,
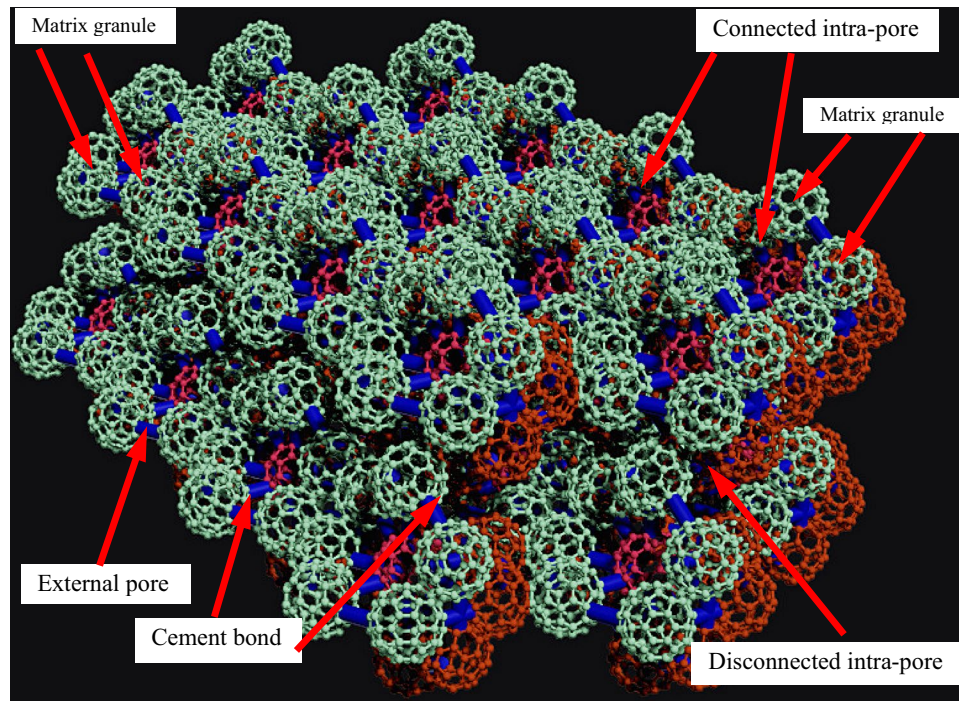
Figure 12. A structural-physical hypothetical model of calcareous sand.

acicular aragonite, and red algae. Previous studies have revealed an abundance of internal pores within calcareous sand particles[11,16]. According to this analysis, this study aimed to propose a hypothetical structural-physical model of calcareous sand, as illustrated in Fig. 12. Different mineral components comprised the particle matrix, and distinct matrix cementation processes generated the disconnected pores within the particles. The variation in the cementation levels between the matrices led to the formation of external pits on the particles. The breakage of cementation bonds between matrices or incomplete cementation achieved the formation of the connected pores within the particles. When subjected to an external force, the cementation bonds between the matrices were disrupted, releasing the internal pores. Subsequently, the fragmented small matrices were connected to smaller matrices through cementation bonds. This phenomenon explained why the external surface of the particles also contained pores when examined under high magnification with SEM after the particle crushing, even for the particles smaller than 0.074 mm. Because of this structural-physical composition and cementation method, the particles exhibited low strength. The cementation bonds are easily broken, which could be one reason for the overall low strength of the calcareous sand.

Quantitative analysis by digital imaging

Although a hypothetical structural-physical model was proposed, the quantitative description of the calcareous sand shape remained elusive. By employing the digital image processing technology, a method for the medium identification and reconstruction was developed. This involved utilizing a mathematical model to identify the medium characteristics and constructing a numerical model based on pixel-unit correspondence. This study was conducted based on the geotechnical tests. Given the limited number of particles larger than 5 mm, only the geometric information for particles smaller than 5 mm is presented in Fig. 13. As shown in Fig. 13, the particles exhibited a generally normal distribution of shape parameters for the same particle size, with each statistical parameter curve demonstrating a consistent trend and minimal dispersion. This suggested a certain degree of reliability in the selected test specimens.

To further quantify the trend of the particle shape variation across different sizes, Fig. 14 presents the statistical graphs illustrating the shape parameters for each particle size category. Generally, the global profile factor and angularity of particles were significantly influenced by size variations. As the particle size increased, the global profile factor decreased and the angularity increased. The dividing lines of flatness, surface roughness, and circularity were particle sizes of 5 mm. For the particle smaller than 5 mm, the size had a notably minimal impact on these characteristics, with the values for each parameter exhibiting a greater concentration. Conversely, for the particles larger than 5 mm, the increases in size were associated with slight increases in the flatness and surface roughness, slight decreases in the circularity, and greater numerical dispersion for each parameter. The comparison of the cumulative graphs suggested that the global profile factor and angularity tend to converge around 1.0 when the particle was small. The surface roughness was approximately 1.2, and the flatness was approximately 1.4, with circularity showing relatively dispersed values around 0.8. As the particle size increased, the global profile factor and circularity decreased, while the flatness, surface roughness, and angularity increased, along with an increase in the numerical dispersion for each parameter. This trend suggested that as the particle size
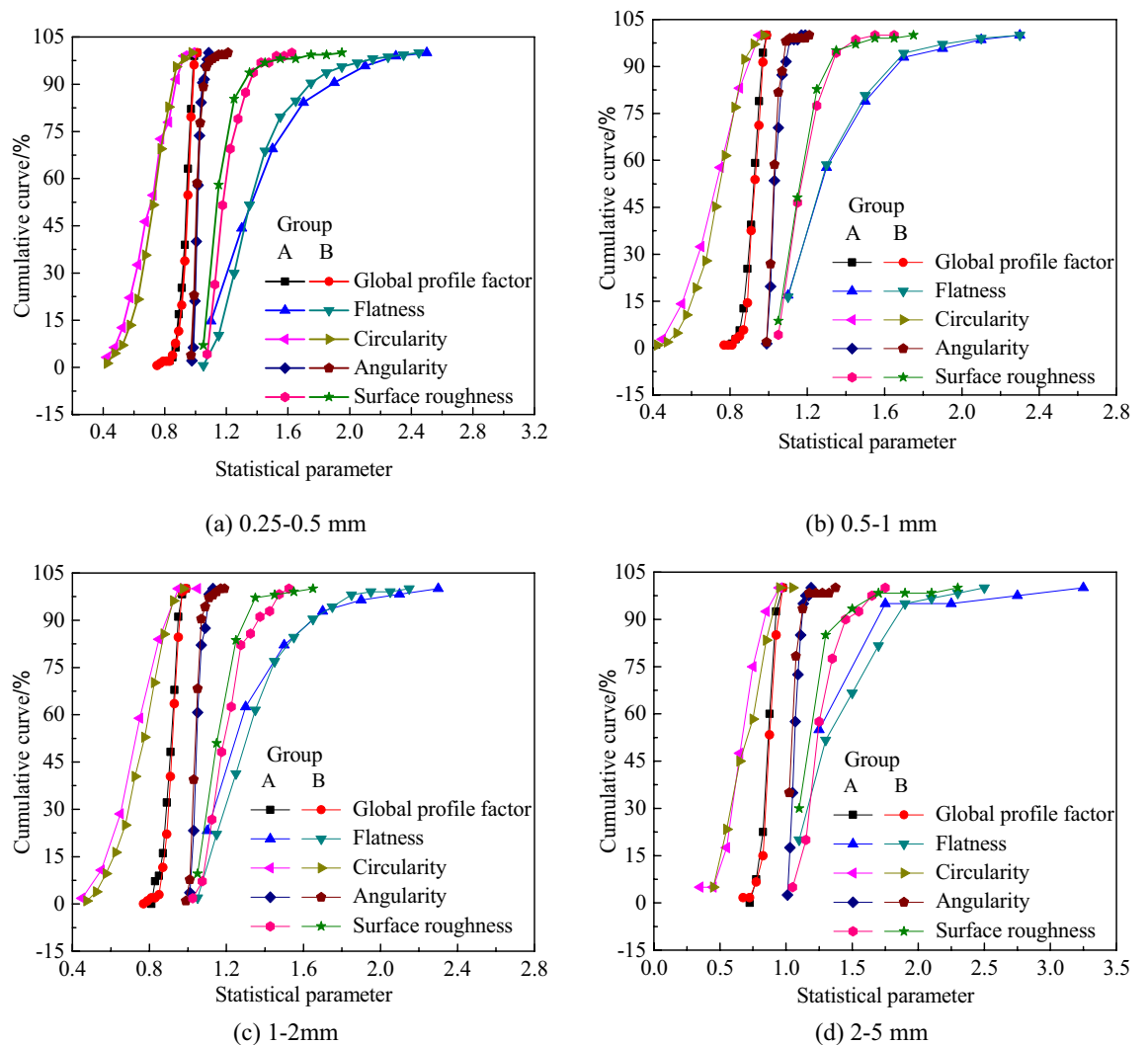
Figure 13. Cumulative curves of statistical parameters for each particle size. (**a**) 0.25–0.5 mm (**b**) 0.5–1 mm (**c**) 1–2 mm (**d**) 2–5 mm.

increased, the particle angles, surface roughness, irregularity, and boundary undulation gradually intensified. The flattening and narrowing characteristics of the particles became increasingly evident, and the shape of the particles became increasingly irregular.

The relationship between the single-particle self-similarity fractal dimension and the particle size is shown in Fig. 14f. For the particles sized from 0.5 to 2 mm, the self-similarity fractal dimensions were primarily concentrated in the range between 1.05 and 1.075. In the 2–5 mm range, fractal dimension served as the transitional phase. For the particles larger than 5 mm, fractal dimensions were slightly smaller, approximately from 1.01 to 1.04. This indicated that the calcareous sand particles did not exhibit the identical fractal dimensions across all scales, suggesting that the particle fractals did not strictly adhere to the self-similarity, as defined by a system of iterated functions. The variation in the single-particle self-similarity fractal dimension was minimal, indicating the presence of the self-similarity random fractal within a specific statistical range. This phenomenon arose because the natural fractals typically adhered to a statistical form of self-similarity rather than the strict self-similarity, where the entirety and its constituent parts exhibited the statistical rather than precise similarities.

In this study, the fractal dimensions of the particles were statistically analyzed using the fixed-scale method to verify the aforementioned conjecture. The analysis was conducted on the data processed from the aforementioned images. Double logarithmic curves were adopted to fit the perimeter L and area A for the four particle size groups: 2–5 mm, 1–2 mm, 0.5–1 mm, and 0.25–0.5 mm. The statistical fractal dimension results for the particles in each size group obtained by analyzing the fitting results are listed in Table 2. The calcareous sand particles demonstrated superior statistical fractal characteristics, with the correlation coefficients of fractal dimension calculation curves for each size group exceeding 90%. The fractal dimensions ranged from 1.04 to 1.07, signifying consistent statistical fractal characteristics of the particle shapes. This suggested that the mineral particles were dispersed as fine particles. When larger mineral particles were decomposed into smaller ones, they maintained fractal dimension of the original larger particles. The constancy of the particle shape fractal dimension despite the particle breakage resulted from the self-similar nature of particle breakage.
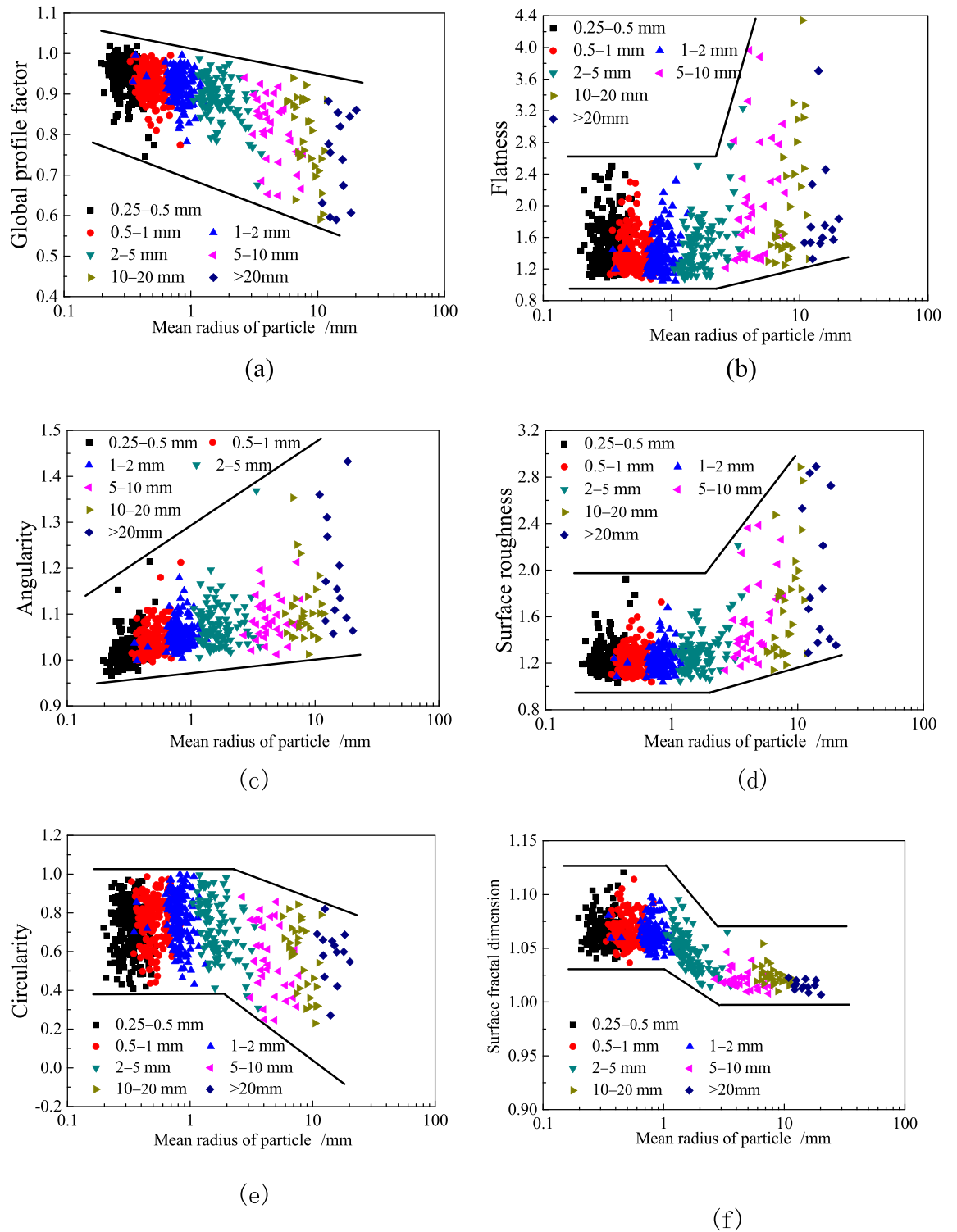
Figure 14. Statistics of particle shape parameter-particle radius.

Particle size	Slope	Fractal dimension	Correlation coefficient
2–5 mm	0.53416	1.06832	0.966
1–2 mm	0.53182	1.06364	0.930
0.5–1 mm	0.53024	1.06048	0.964
0.25–0.5 mm	0.51761	1.03622	0.962

Table 2. Statistics of particle fractals.
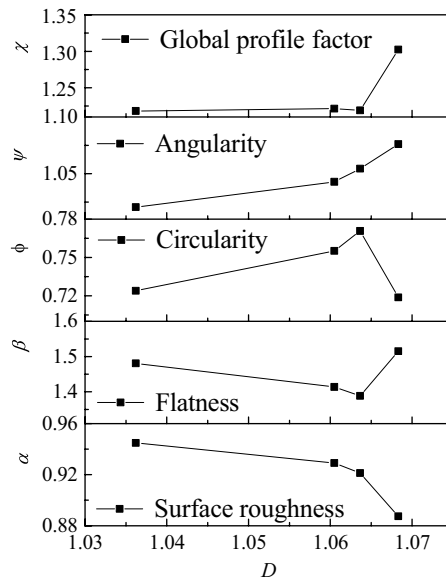
Figure 15. Fractal dimension versus each shape parameter.

The relationship between fractal dimension and particle size followed a certain pattern. The fractal dimension tended to increase as the particle size increased, indicating a specific correlation between them. As shown in Fig. 13, the shape parameters of the individual particles generally exhibited a normal distribution. Therefore, the average value of each shape parameter effectively represented the particle size characteristics. Figure 15 illustrates the relationship between fractal dimensions and average values of the particle shape parameters. As fractal dimension increased, there was consistent variation in the global profile factor, angularity, and surface roughness, all of which presented strong correlations with each other.

Figure 15 demonstrates the following results. First, fractal dimension served as a measure of particle surface smoothness, providing a quantitative assessment of the graph complexity or curvature of the particle contour lines. This dimension reflected the particle morphology in a specific direction. Consequently, as the particle size decreased, the surface smoothness increased. Additionally, the concavity and convexity of the particle surface projected contour line was smaller, and the fractal dimension decreased from the direction greater than 1. The angularity and surface roughness also decreased beyond this value, and the global profile factor tended towards 1 below a value of 1. Second, fractal dimension indicated the extent of particle breakage. The particle breakage can be explained by the physical transformation of large to small particles. Given the slight variance in the fractal dimensions among the particles, it served as a theoretical measure for quantifying the particle breakage. With increased stress, the particle breakage was intensified. There were more particles of small particle size, with lower fractal dimension. Third, fractal dimension correlated with the particle strength, particularly in brittle materials, which typically featured numerous pores and defects of varying sizes. According to the previous structural-physical model, the structure of the material arose from the matrix growth and expansion facilitated by cementation bonds. The macroscopic phenomenon was characterized by the size effect of the particles. The larger particle sizes corresponded to the higher fractal dimensions and lower average particle strength. This was due to the larger particle size, the fractal dimension was higher, the concavity and convexity of the projected contour lines on the particle surface were greater, and there were more cracks and pores in the particles. These contributed to lower particle strength. Finally, All the structural-physical models of the calcareous sand exhibited fractal characteristics. Although the structures of particles with different sizes did not strictly adhere to fractal characteristics, they exhibited the statistical fractal properties, suggesting the presence of self-similarity across different particle sizes.

Notably, since this study adopts a two-dimensional method to quantify the particle shape of calcareous sand, which is limited by the measurement method (the two-dimensional particle morphology is relatively simple, and only needs to obtain the projections and outer contour lines of the particles), may resulting in a certain amount of error in the process of quantifying the particle shape. Compared to the two-dimensional image analysis, analyzing the particle morphology from a three-dimensional perspective required the sophisticated instrumentation to obtain the parameters such as thickness, surface area, and volume. The three-dimensional morphology parameters were derived from the adjustments to the two-dimensional particle morphology parameters. This study applied the two-dimensional method to quantify the particle morphology owing to the technological and equipment limitations. This could be acknowledged as a limitation. Future research will focus on quantifying the three-dimensional shape parameters of the particles.

Conclusion

The calcareous sand specimens from the Yongshu Reef flat in the South China Sea were subjected to SEM and conventional statistical analysis. The shape distribution of particles of various sizes was analyzed using SEM and digital images. The primary findings of this study are as follows.

(1) The calcareous gravel particles exhibited the interwoven reticulation on their surfaces with an uneven distribution of pores. As the particle size decreased, the differences in shape exhibited a decreasing trend and the angularity decreased gradually. A physical model of the results was proposed by integrating the compositional analysis of calcareous sand with basic petrographic knowledge.

(2) As the particle size increased, the global profile factor of the particles decreased, and the angularity increased. A particle size of 5 mm was adopted to identify the thresholds for flatness, surface roughness, and circularity. For the particles smaller than 5 mm, the particle size had a minimal impact on the flatness, surface roughness, and circularity.

(3) As the particle size increased, the fractal dimension also increased. The particle structures across various sizes did not strictly adhere to fractal characteristics. They indicated the statistical fractal characteristics, implying the self-similarity across different sizes. Fractal dimensions served as the indicators of the smoothness and breakage of the particle surface.

Data availability

The data used in this study are provided by the corresponding author upon request.

References

1. Liu, X., Li, S., Yin, F. H. & Yao, T. Morphological characteristics of carbonate soil in South China Sea based on dynamic image technology. *Chin. J. Geotech. Eng.* **45**(3), 590–598 (2023).
2. Luo, M. X., Zhang, J. R., Liu, X. X. & Wu, C. Effect of particle breakage and interlocking on strength and dilatancy characteristics of calcareous sands. *KSCE J. Civ. Eng.* **27**, 3270–3284 (2023).
3. Cho, C. C., Dodds, J. & Santamarina, J. C. Particle shape effects on packing density, stiffness, and strength: Natural and crushed sands. *Geotech. Geoenviron. Eng.* **132**(5), 591–602 (2006).
4. Koerner, R. M. *The behavior of cohesionless materials formed from various materials* (Duke University, 1968).
5. Hyslip, J. & Vallejo, L. Fractal analysis of the roughness and size distribution of granular materials. *Eng. Geol.* **48**(3), 231–244 (1997).
6. Zhu, C. Q., Wang, X. Z., Wang, R., Chen, H. Y. & Meng, Q. S. Experimental microscopic study of inner pores of calcareous sand. *Mater. Res. Innov.* **18**(sup2), 207–214 (2014).
7. Zhu, C. Q., Chen, H. Y., Meng, Q. S. & Wang, R. Microscopic characterization of intra-pore structures of calcareous sands. *Rock Soil Mech.* **35**(07), 1831–1836 (2016).
8. Wang, Y. Q. *Micro-and macro-mechanical behavior of calcareous sand and discrete element method analysis*. Master's thesis, Zhejiang:Zhejiang University (2016).
9. Jiang, L. *The study on particle breakage mechanics characteristics of south China sea calcareous sand*. Master's thesis, Chengdu: Chengdu University of Technology (2014).
10. Chen, H. Y. *Study of the inner pore in calcareous sand*. Master's thesis, Wuhan: Wuhan Institute of Rock and Soil Mechanics, Chinese Academy of Sciences (2005).
11. Chen, H. Y., Wang, R., Li, J. G. & Zhang, J. M. Grain shape analysis of calcareous soil. *Rock Soil Mech.* **26**(9), 1389–1392 (2005).
12. Alshibli, K. A., Druckrey, A. M., Al-Raoush, R. I., Weiskittel, T. & Lavrik, N. V. Quantifying morphology of sands using 3D imaging. *J. Mater. Civ. Eng.* **27**(10), 04014275 (2014).
13. Jiang, M. J., Wu, D., Cao, P. & Ding, Z. J. Connected inner pore analysis of calcareous sands using SEM. *Chin. J. Geotech. Eng.* **39**(S1), 1–5 (2017).
14. Zhou, B., Wang, J. & Wang, H. Three-dimensional sphericity, roundness and fractal dimension of sand particles. *Géotechnique* **68**(1), 18–30 (2018).
15. Wang, B. X. Y. *et al.* Quantitative experimental study of the morphology of coral sand and gravel particles under multiple projection surfaces. *Rock Soil Mech.* **40**(10), 3871–3878 (2019).
16. Li, H. Y., Chai, H. W., Xiao, X. H., Huang, J. Y. & Luo, S. N. Fractal breakage of porous carbonate sand particles: Microstructures and mechanisms. *Powder Technol.* **363**, 112–121 (2020).
17. Cui, X. *et al.* Study on the microscopic characteristics of the three-dimensional pores in coral sand. *Rock Soil Mech.* **41**(11), 3632–3696 (2020).
18. Fu, R., Hu, X. L., Zhou, B., Wang, H. B. & Wang, J. F. A quantitative characterization method of 3D morphology of sand particles. *Rock Soil Mech.* **39**(2), 483–490 (2018).
19. Santamarina, J. C., Cho, G. C. Soil behaviour: The role of particle shape. Advances in Geotechnical Engineering: The Skempton Conference. London, UK: Thomas Telford Publishing, 604–617 (2004).
20. Mitchell, J. K. & Soga, K. *Fundamentals of soil behavior* (John Wiley & Sons, 2005).
21. Arasan, S., Hasiloglu, A. S. & Akbulut, S. Shape properties of natural and crushed aggregate using image analysis. *Int. J. Civ. Struct. Eng.* **1**(2), 221–233 (2010).
22. Maroof, A., Mahboubi, A., Noorzad, A. & Safi, Y. A new approach to particle shape classification of granular materials. *Transp. Geotech.* **22**, 100296 (2020).
23. Maroof, A., Mahboubi, A. & Noorzad, A. A new method to determine specific surface area and shape coefficient of a cohesionless granular medium. *Adv. Powder Technol.* **31**, 3038–3049 (2020).
24. Krumbein, W. C. Measurement and geological significance of shape and roundness of sedimentary particles. *SEPM J. Sediment. Res.* **11**, 64–72 (1941).
25. Powers, M. C. A new roundness scale for sedimentary particles. *SEPM J. Sediment. Res.* **23**, 117–119 (1953).
26. Zhu, C. Q. & Liu, C. Q. Engineering behaviors of coral sands at Yongxing of Xisha Islands. *Rock Soil Mech.* **16**(2), 35–41 (1995).

Acknowledgements

Author contributions

Xiaobing Wei and Yani Lu performed the building plan. Li Zhong and Mingxing Luo performed the specimen preparation and conducted the tests. Xiaoxuan Liu, Biwen Zhang and Li Zhong conducted the discussions. Xiaobing Wei and Li Zhong performed the data analysis and wrote the manuscript.

Competing interests

The authors declare no competing interests.

Additional information

Correspondence and requests for materials should be addressed to X.W. or L.Z.

Reprints and permissions information is available at www.nature.com/reprints.

Publisher's note Springer Nature remains neutral with regard to jurisdictional claims in published maps and institutional affiliations.